EPJ E
Soft Matter and Biological Physics
EPJ.org
your physics journal

Eur. Phys. J. E (2015) **38**: 98 DOI 10.1140/epje/i2015-15098-y

A molecular model for the free energy, bending elasticity, and persistence length of wormlike micelles

Meisam Asgari

edp sciences Società Italiana di Fisica Springer

Eur. Phys. J. E (2015) **38**: 98
DOI 10.1140/epje/i2015-15098-y

THE EUROPEAN PHYSICAL JOURNAL E

Regular Article

A molecular model for the free energy, bending elasticity, and persistence length of wormlike micelles

Meisam Asgari[a]

Department of Mechanical Engineering, McGill University, 817 Sherbrooke Street West, Montreal, QC H3A0C3, Canada

Received 12 February 2015 and Received in final form 15 July 2015
Published online: 15 September 2015 –

Abstract. An expression for the elastic free-energy density of a wormlike micelle is derived taking into account interactions between its constituent molecules. The resulting expression is quadratic in the curvature and torsion of the centerline of micelle and thus resembles free-energy density functions for polymer chains and helical filaments such as DNA. The model is applied on a wormlike micelle in the shape of a circular arc, open or closed. Conditions under which linear chains in dilute systems transform into toroidal rings are analyzed. Two concrete anisotropic soft-core interaction potentials are used to calculate the elastic moduli present in the derived model, in terms of the density of the molecules and their dimensions. Expressions for the persistence length of the wormlike micelle are found based on the flexural rigidities so obtained. Similar to previous observations, our results indicate that the persistence length of a wormlike micelle increases as the aspect ratio of its constituent molecules increases. A detailed application of the model on wormlike micelles of toroidal geometry, along with employing statistical-thermodynamical concepts of self-assembly is performed, and the results are found to be well consistent with the literature. Steps to obtain the material parameters through possible experiments are discussed.

1 Introduction

A surfactant molecule consists of two main parts: a hydrophobic tail and a polar hydrophilic head-group. When present in solution at sufficiently high concentrations, surfactant molecules self-assemble into various supramolecular structures that shield the hydrophobic tails from contact with the ambient solution [1,2]. These structures include spherical micelles, short cylindrical micelles, long cylindrical micelles called wormlike micelles, bilayers, and closed bilayers or vesicles [3,4]. A collection of spherical micelles may undergo uniaxial growth and coalesce into short rodlike cylindrical micelles [5,6]. The ends of a cylindrical micelle are capped by hemispheres [7]. Adding more molecules at certain temperatures and osmotic pressures leads to the formation of wormlike micelles [8,9]. The energy required to create two end caps from a very long cylindrical micelle is called the scission energy [10]. If this energy is sufficiently large and the volume fraction of the surfactant molecules is sufficiently low, the semiflexible micelles may fuse to minimize the number of end caps [3].

In recent years, considerable attention has been paid to investigating the rheological properties of surfactant-based micellar solutions [11–13]. Some examples include soap solutions including micellar globules and adhesives formulated with block copolymers [14]. Due to their novel properties, micellar solutions have found applications as heat transfer fluids, hard-surface cleaners, liquid dish-washing detergents, drag-reducing agents in pipelines, and fracking fluids [15–17]. Such solutions are also useful in biological fields such as targeted diagnostic and therapeutic applications and drug delivery [18–21].

Wormlike micelles may be regarded as mesopolymers since they impart elasticity [22,23] and are subject to breaking and re-shaping [24–26]. They may also become entangled or form branched structures [27]. As a result, a solution in which they are suspended may have viscoelastic behaviour [16,28–30]. For this reason, many rheologists focus on understanding the effective non-Newtonian behaviour of micellar solutions [31,32]. That behaviour is generally influenced by micro-structural changes that occur during flow [33]. The present paper focuses on the energetics of an individual closed or open wormlike micelle, leaving aside questions related to dissipative interactions in flowing solutions.

Wormlike micelles are often characterized by their persistence length. This quantity can be obtained from the bending free energy [34,35]. The free-energy density therefore has a significant role in studying these materials. May *et al.* [36] considered the extent to which the bending elasticity of wormlike micelles influences their tendency to join and form branched structures. In their work, the

[a] e-mail: meisam.asgari@mail.mcgill.ca

free-energy density of a wormlike micelle is comprised of the chain conformational free energy, the end cap energies, and the hydrocarbon-water interfacial energy. Their findings indicate that the energy change associated with the formation of a junction between one micellar end cap and the cylindrical body of another micelle is small relative to the free energy of an end cap.

The first proposed conformational free-energy density function for a wormlike micelle was motived by the Canham-Helfrich [37,38] elastic free-energy density for a lipid vesicle,

$$\psi_{\mathcal{S}} = \gamma_\circ + k_c(H - H_\circ)^2 + \bar{k}_c K, \tag{1}$$

where $\gamma_\circ$ is the surface tension, H and K are the mean and Gaussian curvatures of the surface, k_c and $\bar{k}_c$ are the splay and saddle-splay moduli, and $H_\circ$ is the spontaneous mean curvature, namely the mean curvature of the natural, local shape of the bilayer that has been attributed to the difference between the volumes of the head and tails [39]. The free-energy density $\psi_{\mathcal{S}}$ in (1) has the dimension of energy per *unit area*.

Lauw *et al.* [40] used self-consistent field theory to estimate the free-energy of a closed toroidal wormlike micelle comprised of nonionic surfactant molecules. This relied on specializing the Helfrich expression (1) to a toroidal geometry. Proceeding similarly, Bergström [41,42] investigated the effect of the splay modulus on the size and shape of toroidal micelles and their stability.

An alternative approach to express the free energy of a wormlike micelle is based on the well-established molecular-statistical perspective for modeling self-assembled aggregates. In such an approach, the free energy per amphiphile is considered as the sum of various contributions including hydrophobic effect, chain conformational entropy, electrostatic effects (obtained from linearized Poisson-Boltzmann equation), and head-group repulsion [36,43,44]. According to Bergström [45], the aforementioned contributions can be accurately described by applying Helfrich's curvature elasticity theory.

Wormlike micelles have diameters on the order of 3-5 nanometers. The contour length of a wormlike micelle need not be fixed and may be sensitive to environmental conditions. The length of a wormlike micelle may be extremely large relative to its cross-sectional diameter, reaching 3600 nanometers [15] or as much as one millimeter [22,46]. The ratio of the length of a polymer chain to its thickness can be up to 500 or more [47]. The same ratio for a typical human hair ranges between 10^2 and 10^4. The length-to-diameter ratio of a wormlike micelle exceeds the aforementioned ratios for polymer chains or human hair. Considering the geometric analogy between wormlike micelles and polymer chains, and the application of rodlike models for polymer chains [48,49], an approach closer to those used to model polymers seems to be worthy of consideration.

As previously mentioned, the notion of free-energy density is central to the study of wormlike micelles. For instance, with an expression for the free-energy density of such a micelle, equilibrium configurations can be explored. Here, a free-energy density function is derived for wormlike micelles. To do so, an approach based on accounting for the interactions between the constituent molecules of the micelle is adopted. This approach is largely based on ideas developed by Keller and Merchant [50], who showed that the surface energy of a substance generally includes a bending term and, thus, that the surface may exhibit elastic resistance to bending even in the absence of stretching. This contribution to the free energy is obtained in terms of the molecular density and interaction potential. In a recent application of the work of Keller and Merchant [50], Seguin and Fried [51] derived the Canham-Helfrich free-energy density for a lipid vesicle. In so doing, they modeled the lipid molecules comprising the vesicle by one-dimensional rigid rods. For simplicity, they neglected molecular tilt relative to the orientation of the bilayer. Using the same approach, Asgari and Biria [52] derived the free energy of the edge of an open lipid bilayer based on the interactions between its constituent molecules.

To determine the free-energy density of a wormlike micelle at a position $\mathbf{x}$, we account for the interactions between all surfactant molecules within a cutoff distance d from the molecules at $\mathbf{x}$. For simplicity, we model surfactant molecules as one-dimensional rigid rods and assume that these rods are perpendicular to the centerline of the wormlike micelle. Additionally, interactions between the surfactant molecules comprising the wormlike micelle and the surrounding solution are neglected. Our derivation relies on a Taylor series expansion with respect to a dimensionless parameter $\delta := d/\ell \ll 1$, where ℓ is the smallest radius of curvature that the centerline of a wormlike micelle is capable of exhibiting. The free energy of an open wormlike micelle results on integrating this density over the centerline of the wormlike micelle and adding the end cap energies.

This article is organized as follows: In sect. 2, modeling assumptions and geometrical considerations are briefly presented. The section is followed by introducing the distribution function of the molecules along the body of the wormlike micelle. Section 3 includes the calculation of the free-energy density along the tubular body of the wormlike micelle, followed by obtaining the free energy of closed and open wormlike micelles. Section 4 is concerned with the application of the model to a wormlike micelle in the shape of a circular arc, open or closed. The consequences of choosing a spheroidal particle potential [53,54], and the interaction potential to be of the form proposed by Lintuvuori and Wilson [55] are considered in sect. 5, to calculate the elastic moduli and persistence length of wormlike micelles. Section 5 is followed by making connections between our results and previous experimental observations. A detailed application of the model on wormlike micelles of toroidal geometry along with applying statistical-thermodynamical concepts of self-assembly, and suggested experimental procedure towards obtaining the material parameters, are provided in sect. 6. Finally, the key findings and implications of this study are summarized and discussed in sect. 7. Details of the various derivations are presented in appendix A.

2 Modeling assumptions

According to the assumptions below, the body of a wormlike micelle is envisioned as a tubular domain with centerline $\mathcal{C}$ of length L, and constant cross-sectional radius ξ:

1) The surfactant molecules that comprise the micelle have identical physiochemical properties.
2) Each surfactant molecule can be modeled as a one-dimensional rigid rod of length ξ.
3) The surfactant molecules at any point of $\mathcal{C}$ are arranged perpendicular to $\mathcal{C}$ with a uniform angular distribution.
4) The length L of the wormlike micelle far exceeds its radius ξ, namely the length ξ of a single molecule.
5) The minimum radius of curvature that a wormlike micelle can support at each point is denoted by ℓ. This characteristic length is assumed to be large relative to the length ξ of a single molecule.

As a consequence of assumptions 2) and 3), the head-groups of surfactant molecules lie on a tubular surface of constant circular cross-section. Assumption 3) is based on the observation that the hydrophobic tails of surfactant molecules are oriented (on average) along the normal of the tubular interface [36, 56]. Assumption 4) allows the wormlike micelle to be identified with its centerline $\mathcal{C}$. Assumption 5) refers to the fact that the tubular body of the micelle may adopt various shapes; however, being made up of molecules of a finite size, it cannot support arbitrarily large curvatures. Moreover, the tubular body does not overlap (or even contact) itself. On this basis, there is an upper bound for the curvature (or, equivalently, a lower bound for the radius of curvature) which ensures that contact/overlap does not occur. We denote such radius of curvature by ℓ. This parameter is assumed to be much larger than molecular dimensions.

2.1 Preliminary geometrical considerations

Let $\mathcal{C}$ denote the centerline of the tubular domain that represents the wormlike micelle and consider an arclength parametrization

$$\mathcal{C} = \{\mathbf{x} : \mathbf{x} = \mathbf{x}(s),\ 0 \le s \le L\}. \tag{2}$$

Using a prime to denote differentiation with respect to the arclength s, it follows that

$$|\mathbf{x}'| = \left|\frac{\mathrm{d}\mathbf{x}}{\mathrm{d}s}\right| = \left(\frac{\mathrm{d}\mathbf{x}}{\mathrm{d}s}\cdot\frac{\mathrm{d}\mathbf{x}}{\mathrm{d}s}\right)^{1/2} = 1 \tag{3}$$

and, also, that

$$\mathbf{x}'\cdot\mathbf{x}'' = 0, \qquad \text{and} \qquad |\mathbf{x}'\times\mathbf{x}''| = |\mathbf{x}''|. \tag{4}$$

The unit tangent $\mathbf{t}$, unit normal $\mathbf{n}$, and unit binormal $\mathbf{b}$ of the Frenet frame $\{\mathbf{t}, \mathbf{n}, \mathbf{b}\}$ of $\mathcal{C}$ are given in terms of the arclength parametrization $\mathbf{x}$ of $\mathcal{C}$ by (fig. 1)

$$\mathbf{t} = \mathbf{x}', \qquad \mathbf{n} = \frac{\mathbf{x}''}{|\mathbf{x}''|}, \qquad \text{and} \qquad \mathbf{b} = \frac{\mathbf{x}'\times\mathbf{x}''}{|\mathbf{x}''|}. \tag{5}$$

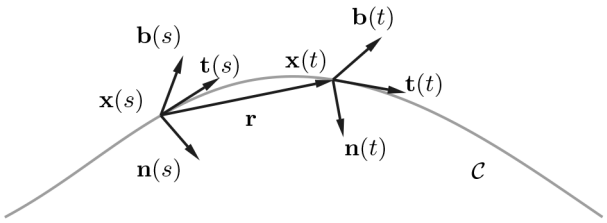

Fig. 1. Two positions $\mathbf{x}(s)$ and $\mathbf{x}(t)$ on the centerline of a wormlike micelle with the intermolecular vector $\mathbf{r}$, and the Frenet frame at those positions.

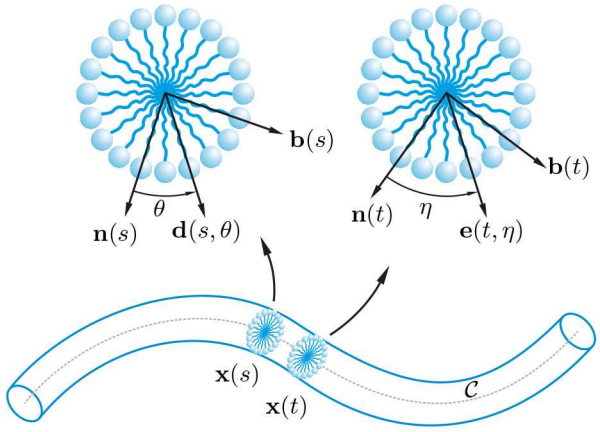

Fig. 2. Geometry of a part of the tubular body of a wormlike micelle based on simplifying assumptions. The head-groups of the molecules at $\mathbf{x}(s)$ must lie on the boundary of a disk (of radius ξ) in the plane spanned by $\mathbf{n}(s)$ and $\mathbf{b}(s)$.

Moreover, the curvature κ and torsion τ of $\mathcal{C}$ are given by

$$\kappa = |\mathbf{t}'| = |\mathbf{x}''|, \qquad \text{and} \qquad \tau = \pm|\mathbf{b}'| = \frac{\mathbf{x}'\cdot(\mathbf{x}''\times\mathbf{x}''')}{|\mathbf{x}''|^2}. \tag{6}$$

Let s belong to the interval $(0, L)$, so that $\mathbf{x}(s)$ is interior to $\mathcal{C}$. Consider a molecule at the position $\mathbf{x}(s)$ with orientation θ measured counterclockwise from the line determined by the unit normal $\mathbf{n}(s)$. The director of this molecule is given by the unit vector $\mathbf{d}(s, \theta)$. According to assumption 3), the director $\mathbf{d}(s, \theta)$ of the molecule at $\mathbf{x}(s)$, can be expressed as a linear combination

$$\mathbf{d}(s, \theta) = (\cos\theta)\,\mathbf{n}(s) + (\sin\theta)\,\mathbf{b}(s), \tag{7}$$

of unit normal $\mathbf{n}(s)$ and unit binormal $\mathbf{b}(s)$ (fig. 2). Similarly, the director $\mathbf{e}(t, \eta)$ of the molecule at position $\mathbf{x}(t)$ can be expressed as a linear combination of $\mathbf{n}(t)$ and $\mathbf{b}(t)$ by (fig. 2)

$$\mathbf{e}(t, \eta) = (\cos\eta)\,\mathbf{n}(t) + (\sin\eta)\,\mathbf{b}(t). \tag{8}$$

2.2 Molecular distribution function

The way that surfactant molecules are distributed along the tubular body of the wormlike micelle has an effect

in describing how such molecules interact. The molecular distribution function describes how such molecules are distributed along $\mathcal{C}$.

The distribution of the molecules at a generic point s in the open interval $(0, L)$ along $\mathcal{C}$ is denoted by $f > 0$. It follows that the integral

$$\int_0^L \int_0^{2\pi} f(s)\,\mathrm{d}\theta\,\mathrm{d}s \tag{9}$$

represents the total number of surfactant molecules comprising the tubular body of the wormlike micelle. In view of assumption 3) the angular distribution of surfactant molecules alone $\mathcal{C}$ is uniform. Consequently, (9) yields

$$2\pi \int_0^L f(s)\,\mathrm{d}s. \tag{10}$$

3 Free energy of a wormlike micelle

Wormlike micelles are either closed or open. An open wormlike micelle possesses two end caps. Branched wormlike micelles, however, possess more than two end caps along with junctions which may contribute additional free energy [9,57]. Here, we first derive the free-energy density on the body of the wormlike micelle. The net free-energy of a closed wormlike micelle is simply found by integrating the derived free-energy density over the body of the micelle. For an open wormlike micelle, the free energy corresponding to the end caps should be added to the net free energy of the body. For simplicity, we restrict attention to wormlike micelles that do not possess branches and, thus, possess only two end caps.

The equilibrium between open and closed wormlike micelles of a given length is determined by the difference between their free energy. When an open wormlike micelle is closed to form a ring, two hemispherical end caps are removed. Such removal yields a negative free energy. However, upon such a conformational change, the entropy of the system is reduced yielding a positive free energy [58]. The equilibrium between open and closed wormlike micelles is the consequence of the balance between these two free-energy contributions. In the dilute limit, shorter chains are expected to be linear, and longer ones are expected to be closed rings.

3.1 Free-energy density of the tubular body of the wormlike micelle

The interaction energy between two rodlike structures is based on three ideas, the first of which entails considering the molecules as one-dimensional rigid rods, the second embodies the notion that the rods are made up of material points that interact with each other, and the third being the principle of material frame-indifference, which states that the constitutive relations describing the internal interactions between the parts of a system should not depend on the external frame of reference used to describe them [59]. This principle places restrictions on the constitutive equations.

Assume that the interaction between two molecules is governed by an energy function depending on the location of the two molecules and the directors indicating the orientation of the molecules [51,60]. Consider two molecules at positions $\mathbf{x}(s)$ and $\mathbf{x}(t)$ on $\mathcal{C}$, as depicted schematically in fig. 2. From (7) and (8), their directors are of the form $\mathbf{d}(s,\theta)$ and $\mathbf{e}(t,\eta)$, respectively. Let

$$\Omega\left(\mathbf{x}(s), \mathbf{x}(t), \mathbf{d}(s,\theta), \mathbf{e}(t,\eta)\right), \tag{11}$$

denote the interaction energy between these two molecules. An interaction energy of the form (11) may encompass different effects such as steric or electrostatic interactions between surfactant molecules. Following Keller and Merchant [50], assume that the interaction energy between two molecules separated by a distance greater than some fixed cutoff distance d vanishes. To express this differently, assume that only molecules within a distance d may interact. On denoting the relative position vector between a pair of molecules at $\mathbf{x}(s)$ and $\mathbf{x}(t)$ by $\mathbf{r} = \mathbf{x}(s) - \mathbf{x}(t)$, it follows that Ω satisfies

$$|\mathbf{r}| > d \Longrightarrow \Omega\left(\mathbf{x}(s), \mathbf{x}(t), \mathbf{d}(s,\theta), \mathbf{e}(t,\eta)\right) = 0. \tag{12}$$

It is assumed that the cutoff distance d is small relative to the minimum radius of curvature ℓ introduced in assumption 5), so that $d \ll \ell$ or,

$$\delta := \frac{d}{\ell} \ll 1. \tag{13}$$

Granted that Ω is frame indifferent [59], it must obey

$$\Omega\left(\mathbf{x}(s), \mathbf{x}(t), \mathbf{d}(s,\theta), \mathbf{e}(t,\eta)\right) = 2\,\hat{\Omega}\left(\frac{|\mathbf{r}|^2}{\delta^2}, \mathbf{r}\cdot\mathbf{d}(s,\theta), \mathbf{r}\cdot\mathbf{e}(t,\eta), \mathbf{d}(s,\eta)\cdot\mathbf{e}(t,\eta)\right), \tag{14}$$

where a factor of 2 has been introduced to simplify subsequent calculations. The quantity $\hat{\Omega}$ on the right-hand side of (14) is a function of four scalar arguments. These arguments include the length of the intermolecular vector $\mathbf{r}$, and the dot products $\mathbf{r}\cdot\mathbf{d}$ and $\mathbf{r}\cdot\mathbf{e}$ between the directors and that vector and the dot product $\mathbf{d}\cdot\mathbf{e}$ between the directors. Such dot products are related to the angles α_1 and α_2 between the relative position vector $\mathbf{r}$ and the directors $\mathbf{d}$ and $\mathbf{e}$, and also to the angle α_3 between the two directors $\mathbf{d}$ and $\mathbf{e}$, by

$$\hat{\mathbf{r}}\cdot\mathbf{d} = \cos\alpha_1, \qquad \hat{\mathbf{r}}\cdot\mathbf{e} = \cos\alpha_2, \qquad \mathbf{d}\cdot\mathbf{e} = \cos\alpha_3, \tag{15}$$

with $\hat{\mathbf{r}}$ being the unit vector corresponding to the intermolecular vector $\mathbf{r}$. According to (12), Ω depends implicitly upon d through δ, while $\hat{\Omega}$ does not depend upon d. The term δ^2 in the denominator of the first argument on the right-hand side of (14) is introduced to remove that dependence. It follows from (12)–(14) that $\hat{\Omega}$ satisfies

$$s > \ell \Longrightarrow \hat{\Omega}(s^2, s\delta\cos\alpha_1, s\delta\cos\alpha_2, \cos\alpha_3) = 0. \tag{16}$$

The total free energy $E_{\rm tot}$ of the tubular body of the wormlike micelle is given by

$$E_{\rm tot} = \int_0^L \int_0^L \int_0^{2\pi} \int_0^{2\pi} \frac{1}{2}\Omega\left(\mathbf{x}(s), \mathbf{x}(t), \mathbf{d}(s,\theta), \mathbf{e}(t,\eta)\right) \times f(s) f(t) \mathrm{d}\theta \, \mathrm{d}\eta \, \mathrm{d}t \, \mathrm{d}s. \quad (17)$$

To reiterate, $\Omega(\mathbf{x}(s), \mathbf{x}(t), \mathbf{d}(s,\theta), \mathbf{e}(t,\eta))$ is the interaction energy between a molecule at position $\mathbf{x}(s)$ with orientation $\mathbf{d}(s,\theta)$ and a molecule at $\mathbf{x}(t)$ with orientation $\mathbf{e}(t,\eta)$. Whereas $f(s)$ gives the density of the molecules at $\mathbf{x}(s)$, $f(t)$ gives the same quantity at $\mathbf{x}(t)$. By integrating from 0 to 2π with respect to the variables θ and η, the interaction energy between all of the molecules of the two cross-sections at $\mathbf{x}(s)$ and $\mathbf{x}(t)$ is taken into account. The integrand in (17) is multiplied by $1/2$ because otherwise it double counts the interaction energy between each pair of molecules. By integrating over t from 0 to L, the interaction of all the molecules of the other cross-sections with the molecules located in the cross-section at the position $\mathbf{x}(s)$ is incorporated. The second integration, over s from 0 to L, ensures that the free energy of each cross-section is counted.

The net free-energy function $E_{\rm tot}$ of the tubular body of the wormlike micelle is related to the free-energy density ψ by

$$E_{\rm tot} = \int_0^L \psi \, \mathrm{d}s. \quad (18)$$

By (14)–(17), the free-energy density ψ of the wormlike micelle at a position $\mathbf{x} = \mathbf{x}(t_\circ)$ on $\mathcal{C}$ is, up to an arbitrary additive constant, given by

$$\psi = \int_0^L \int_0^{2\pi} \int_0^{2\pi} \hat{\Omega}\Big(\frac{|\bar{\mathbf{r}}(t)|^2}{\delta^2}, \bar{\mathbf{r}}(t) \cdot \mathbf{d}(t_\circ,\theta), \bar{\mathbf{r}}(t) \cdot \mathbf{e}(t,\eta), \mathbf{d}(t_\circ,\theta) \cdot \mathbf{e}(t,\eta) \Big) f(t_\circ) f(t) \, \mathrm{d}\theta \, \mathrm{d}\eta \, \mathrm{d}t, \quad (19)$$

where $\bar{\mathbf{r}}(t) = \mathbf{x}(t_\circ) - \mathbf{x}(t)$ is the intermolecular vector.

Upon performing the Taylor expansion of the right-hand side of (19) up to two derivatives, the specific steps of which appear in appendix A, the final form of the free-energy density for a wormlike micelle is found to be

$$\psi = \psi_\circ + k_c \kappa^2 + k_t \tau^2, \quad (20)$$

which includes the sum of a quadratic term in curvature κ and a quadratic term in torsion τ of the centerline $\mathcal{C}$ of the micelle, defined in (6). The free-energy density ψ in (20) is independent of the size and shape of the wormlike micelle. Thus, according to our theory, the free energy of a wormlike micelle in an equilibrated system is completely determined by the parameters $\psi_\circ$, k_c and k_t.

The term $\psi_\circ$ in (20) is insensitive to the shape of the wormlike micelle. Since the molecular distribution function f has implicit dependence upon effects like temperature, concentration, and electromagnetic fields, these effects may be encompassed in $\psi_\circ$ and in the moduli k_c and k_t. The role of the term $\psi_\circ$ in (20) is similar to that of $\gamma_\circ$ in Helfrich's free-energy density (1). However, $\gamma_\circ$ in (1) is not an independent parameter, and is determined by the condition of constant overall surfactant concentration [61].

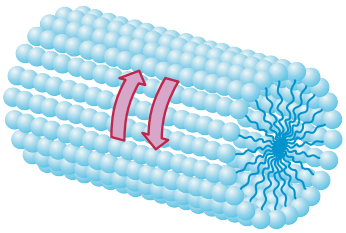

Fig. 3. Schematic of a small section of a wormlike micelle. Since the molecules can rotate freely, no energetic cost in incurred by twisting.

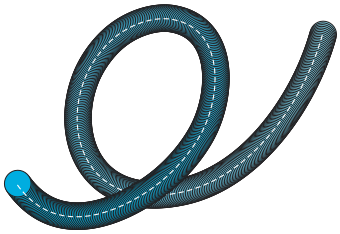

Fig. 4. Schematic of a wormlike micelle that possesses torsion. A curve with null torsion is a planar curve.

The flexural (or bending) rigidity k_c in (20) represents the resistance of the wormlike micelle against deviations from a uniform curvature. It further describes the stability and stiffness of the wormlike micelle [62]. Similarly, the torsional rigidity k_t denotes the resistance of the wormlike micelle against moving out of the osculating plane of the centerline $\mathcal{C}$ at each point. The moduli k_c and k_t depend upon the size and composition of surfactant molecules comprising the micelle, the distribution of the molecules, temperature, and the concentration of the solution [45]. Further, the flexural rigidity k_c in (20) has the dimension of energy times length, and thus, is not the same as the flexural rigidity k_c in the Canham-Helfrich free-energy density (1), which has the dimension of energy.

The torsion τ of $\mathcal{C}$ should not be confused with the twist between different cross sections of $\mathcal{C}$. Since the rod-like molecules comprising the wormlike micelle may adjust their positions in response to the twist between adjacent cross sections, as shown in fig. 3, the expression (19) for the free-energy density ψ contains no contribution related to twist. In contrast, τ measures the turnaround of the binormal $\mathbf{b}$ of $\mathcal{C}$ (which denotes the nonplanarity of $\mathcal{C}$ [63]) or, equivalently, the tendency of $\mathcal{C}$ to move out of a given osculating plane (fig. 4). Thus, τ vanishes for plane curves and is constant for helical curves. As defined in $(6)_2$, τ is positive (negative) for a right-handed (left-handed) helix.

The expression in (20), which is known in the context of the elasticity of bent rods [64], resembles free-energy density functions for polymer chains [48,49,65] and those for DNA [66,67]. However, in contrast to those models, (20) contains evidence of neither intrinsic curvature nor intrinsic torsion. For a wormlike micelle consisting of

more than one type of surfactant molecule, the presence of molecules with different head-group or tail conformations might lead to intrinsic curvature or intrinsic torsion. In the present setting, such effects are ruled out by our first modeling assumption.

3.2 Free energy of a closed wormlike micelle

For a closed wormlike micelle, the centerline $\mathcal{C}$ is closed. Integrating the free-energy density function in (20) over $\mathcal{C}$ yields the total free energy,

$$E_{\text{tot}} = \int_{\mathcal{C}} \left(\psi_\circ + k_c\kappa^2 + k_t\tau^2\right) \mathrm{d}s, \tag{21}$$

of a closed wormlike micelle with centerline $\mathcal{C}$.

3.3 Free energy of an open wormlike micelle

Consider now an open wormlike micelle with two end caps. The net free energy of such a wormlike micelle is obtained by adding the free energy of the tubular body and that of the two end caps. The former is obtained by integrating the free-energy density (20) over $\mathcal{C}$. The latter is obtained by 2 times the free energy E_{cap} corresponding to an end cap. The result is given by the sum

$$E_{\text{tot}} = \int_{\mathcal{C}} \left(\psi_\circ + k_c\kappa^2 + k_t\tau^2\right) \mathrm{d}s + 2E_{\text{cap}}. \tag{22}$$

Wormlike micelles may become much larger than their persistence length, and adopt standard polymer statistics on large scales in which entropy dominates the overall chain configuration, and there is no well-defined elastic reference in such limit [3]. To account for this problem, a high persistence length for the micellar body is assumed in the present study. Further, long-range excluded-volume interactions between the surfactant monomers are not taken into account in our model, which is consistent with the high persistence length assumption [68].

4 Illustrative examples

In this section, we investigate the application of our model on two examples of wormlike micelles, the first of which an open wormlike micelle in the shape of a circular arc, and the second, a closed wormlike micelle in the shape of a torus. Bearing in mind the relatively high difference between the free energy associated with the end caps and that associated with the tubular body of the micelle, we then explore the condition under which the open wormlike micelle in the shape of the circular arc tends to close itself to form a toroidal micelle in a dilute solution.

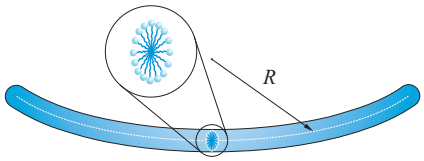

Fig. 5. Schematic of a planar open wormlike micelle in the shape of an arc of a circle.

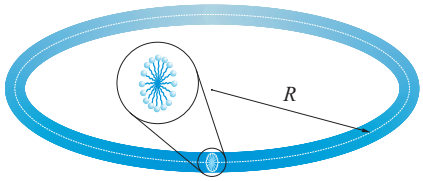

Fig. 6. Toroidal wormlike micelle with constant radius of curvature R.

4.1 Example 1: open wormlike micelle

The length of a wormlike micelle is much greater than its cross-sectional radius, and thus, it can be regarded as a one-dimensional continua. Consider a planar open wormlike micelle in the shape of a circular arc of length $L = R\gamma$, where R and γ respectively denote the radius of curvature and the central angle corresponding to the arc (fig. 5). Assume that the length of the arc is large enough, compared to the cross-sectional diameter of the wormlike micelle, to ensure assumption 4) in sect. 2. Since the torsion τ of a circular arc vanishes, the corresponding net free energy E_{tot} in (22) simplifies to

$$E_{\text{tot}} = \int_0^L \left(\psi_\circ + k_c\kappa^2\right) \mathrm{d}s + 2E_{\text{cap}}. \tag{23}$$

Assuming $\psi_\circ$ and k_c to be uniform along $\mathcal{C}$, while bearing in mind that the curvature κ is $1/R$ along the arc and $\mathrm{d}s = \mathrm{d}\theta/\kappa = R\,\mathrm{d}\theta$, (23) specializes to

$$E_{\text{tot}} = \gamma R \left(\psi_\circ + \frac{k_c}{R^2}\right) + 2E_{\text{cap}}. \tag{24}$$

4.2 Example 2: toroidal wormlike micelle

Consider a closed wormlike micelle in the shape of a torus with the constant major radius R, and the minor radius ξ, as indicated in fig. 6. The length of such a micelle, which is $L = 2\pi R$, is assumed to be large enough relative to the minor radius ξ, so that assumption 4) in sect. 2 holds. Considering the fact that torsion τ for the centerline of a torus vanishes, and $\kappa = 1/R$ along the centerline $\mathcal{C}$ of the torus, while keeping in mind that $\mathrm{d}s = R\,\mathrm{d}\theta$, the total free energy E_{tot} in (21) takes the form

$$E_{\text{tot}} = \int_0^{2\pi} \left(\psi_\circ + \frac{k_c}{R^2}\right) R\,\mathrm{d}\theta. \tag{25}$$

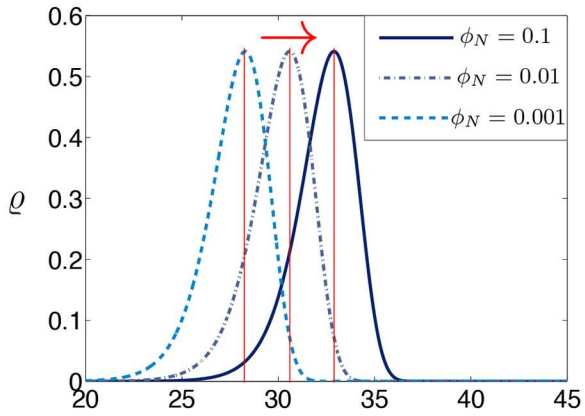

Fig. 7. Plot of the number density ϱ of micellar chains against the free energy $E_{\rm tub}$ of the micellar body for different values of the surfactant volume fraction ϕ_N. At each volume fraction ϕ_N, the maximum number density of chains in the dilute system occurs at a particular value $E^*_{\rm tub}$ of the free energy of tubular body. For chains with $E_{\rm tub} > E^*_{\rm tub}$, the number density of the open chains has a descending trend, showing that in the dilute limit, longer chains are expected to be closed rings. As is evident from the graphs, the chain-ring transition for longer chains increases by increasing surfactant volume fraction in the dilute system.

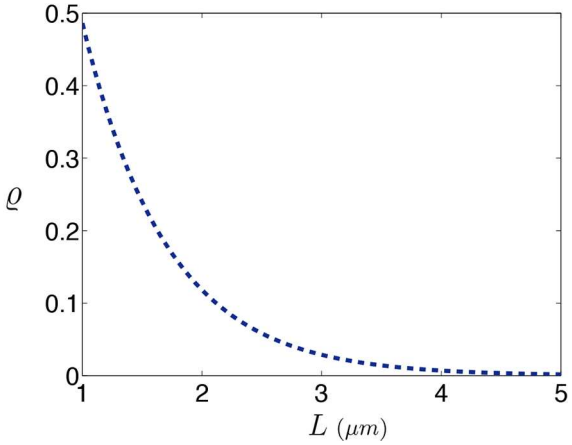

Fig. 8. Plot of the number density ϱ against length L for $\phi_N \ll 1$ (*i.e.*, dilute limit) and for $\mathcal{E} = 10\ k_BT$. As is evident from the plot, in the dilute limit, the number density ϱ of shorter chains is higher than that of longer chains. Thus, in the dilute limit, shorter chains are expected to be linear, and longer ones are expected to be closed.

Assuming $\psi_\circ$ and k_c to be uniform along $\mathcal{C}$, (25) results

$$E_{\rm tot} = 2\pi R\left(\psi_\circ + \frac{k_c}{R^2}\right). \tag{26}$$

Granted that $\psi_\circ$ and k_c are positive, the free-energy functions expressed in (24) and (26) tend to $+\infty$ when R approaches zero or $+\infty$. Also, the second derivative of the functions expressed in (24) and (26) with respect to R are positive. Thus, both functions are convex with respect to R, and each possess a single minimum. As a result, the corresponding equilibrium state for each case is stable. The minimum of the total free energy $E_{\rm tot}$ in (26) occurs at $R^* = \sqrt{k_c/\psi_\circ}$. Thus, our theory predicts that toroidal micelles with constant radius of curvature tend to have the major radius R^* at the equilibrium state.

4.3 A comparison between the two examples: Ring-chain equilibrium in a dilute system

It has been reported that the free energy due to the end caps is relatively high [69, 70]. This relatively high free energy might be due to the way that the surfactant molecules are packed at the ends to form two hemispherical caps, which shield the water from the hydrocarbon chains [69,71]. In a dilute solution at equilibrium, the free energy of a collection of wormlike micelles is minimized by reducing the number of end caps [1]. Under certain conditions, this may be accompanied by elongation of wormlike micelles [72]. Nevertheless, since micelles are made by self-assembly of amphiphiles in a solution, linear chains, rings, and other possible structures compete for the available surfactant monomers in the solution. At equilibrium, it is the free energy of the whole system that should be minimized, and not that of a specific structure. As a consequence of elongation and also the entropic effects, if the bending energy of a closed ring becomes larger than the net free energy of a linear micelle, the chain is expected to open to reach a lower energy. In semi-dilute and dense systems, the population of linear chains increases and ultimately dominates by increasing surfactant density.

The number density ϱ of dilute inflexible wormlike micelles of length L is expressed as [3,73,74]

$$\varrho = \frac{\exp\left(\frac{-L}{L_e}\right)}{L_e^2}, \tag{27}$$

where

$$L_e = \sqrt{\phi_N}\exp\left(\frac{\mathcal{E}}{2k_BT}\right), \tag{28}$$

denotes the entanglement length of the micelle. In (28) ϕ_N denotes the surfactant volume fraction, $k_B = 1.3807 \times 10^{-23}$ N m/K is the Boltzman's constant, T is the absolute temperature, and

$$\mathcal{E} = 2E_{\rm cap} - E_{\rm tub}, \tag{29}$$

denotes the scission energy, which represents the excess energy of a pair of hemispherical end caps to that of the cylindrical interior region [71]. The end cap energy $E_{\rm cap}$ can be obtained by performing a temperature jump experiment [75]. According to Gelbart and Ben-Shaul [69], this energy can be as much as 20 k_BT. In the dilute regime and at certain thermo-mechanical conditions in which the surfactant volume fraction ϕ_N is relatively low, shorter chains are expected to be linear, and longer ones are expected to be rings of toroidal geometry (figs. 7 and 8). Under such

conditions, it becomes energetically favourable for the system to lessen the number of end caps.

Consider the two examples discussed in sects. 4.1 and 4.2. As it transpires, regardless of the change in the free energy due to the conformational entropy, at a specific value $\gamma_{\rm cr}$ of γ, the total free energy $E_{\rm tot}$ of the open wormlike micelle in the shape of the circular arc in (24) becomes greater than the total free energy $E_{\rm tot}$ of the toroidal micelle in (26). At equilibrium, the system prefers the state with the lower free energy. Therefore, for $\gamma > \gamma_{\rm cr}$, the open wormlike micelle in the dilute solution is expected to display a tendency to lose its end caps and form a toroidal micelle; alternatively, the micelle prefers to remain open if γ is smaller than $\gamma_{\rm cr}$. The angle $\gamma_{\rm cr}$ at which this occurs, can be found by equating the right-hand sides of (24) and (26):

$$(2\pi - \gamma_{\rm cr})\left(\frac{k_c}{R} + \psi_\circ R\right) = 2E_{\rm cap}. \tag{30}$$

Hence,

$$\gamma_{\rm cr} = 2\pi - \frac{2R\,E_{\rm cap}}{k_c + \psi_\circ R^2}\,. \tag{31}$$

As noted above, the free-energy contribution due to the entropy loss associated with the ring closure constraint in (30) has been ignored. According to Van Der Schoot and Cates [76] and Porte [77], for the ideal solution in the rigid limit, that term remains small and may be neglected.

5 Application of a specific potential: Calculation of the elastic moduli and persistence length

The present section establishes that the predictions of our developed model agree both qualitatively and quantitatively with prior observations on wormlike micelles.

Various interaction potentials have been introduced to describe the interaction between pairs of rigid elongated axisymmetric molecules. Such interaction potentials take into account the distance between the two molecules and their orientations. Some of these potentials become infinite when the distance between the interacting molecules approaches zero. Such potentials are called hard-core. The Gay-Berne [54] potential, which is an anisotropic generalization of the Lennard-Jones [78] potential, is of the hard-core type. On the other hand, there are soft-core potentials that take a finite value if the two molecules overlap. Two examples of such potentials between rodlike molecules were proposed by Berne and Pechukas [53] and Lintuvuori and Wilson [55]. Since the present model for a wormlike micelle is continuous rather than discrete, only soft-core potentials can be applied on this model. To compute the flexural and torsional rigidities, the interaction between the molecules arbitrarily close together must be taken into account. Thus, considering a hard-core potential would lead to infinite flexural and torsional rigidities. In this section, a spheroidal-particle potential [53,54], and Lintuvuori-Wilson [55] potential are applied to determine explicit expressions for the moduli $\psi_\circ$, k_c and k_t.

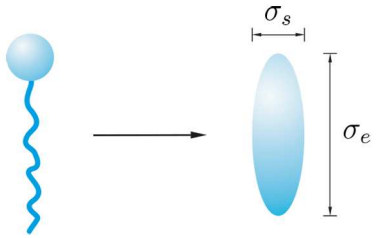

Fig. 9. Schematic of an equivalent ellipsoid of revolution (or spheroid) for the surfactant molecule.

5.1 Spheroidal-particle potential

Some of the available potentials which describe the interaction between axisymmetric rodlike molecules, model such molecules by spheroidal particles, as depicted schematically in fig. 9. Such potentials possess a multiplicative decomposition

$$\hat{\Omega}(\mathbf{r},\mathbf{d},\mathbf{e}) = \hat{\Lambda}(\hat{\mathbf{r}},\mathbf{d},\mathbf{e})\hat{\Gamma}(\mathbf{r},\mathbf{d},\mathbf{e}), \tag{32}$$

where $\hat{\mathbf{r}}$ is the unit vector corresponding to the intermolecular vector $\mathbf{r}$. Also, $\mathbf{d}$ and $\mathbf{e}$ denote the orientations of the two molecules under consideration. In (32), $\hat{\Lambda}$ and $\hat{\Gamma}$ are referred to as the strength and distance parameters, respectively. The strength parameter $\hat{\Lambda}$ does not depend upon the distance between the molecules, whereas, the distance parameter $\hat{\Gamma}$ does. For the strength parameter $\hat{\Lambda}$, the following expression proposed by Gay and Berne [54] is used

$$\hat{\Lambda}(\hat{\mathbf{r}},\mathbf{d},\mathbf{e}) = 4\,\Lambda_\circ \hat{\Lambda}_1(\mathbf{d},\mathbf{e})^\lambda \hat{\Lambda}_2(\hat{\mathbf{r}},\mathbf{d},\mathbf{e})^\mu, \tag{33}$$

where $\Lambda_\circ$ is a fitting parameter, and λ and μ are parameters that specify the type of molecules under consideration. In (33), $\hat{\Lambda}_1$ and $\hat{\Lambda}_2$ are given by

$$\hat{\Lambda}_1(\mathbf{d},\mathbf{e}) = \frac{1}{(1-\chi^2(\mathbf{d}\cdot\mathbf{e})^2)^{1/2}}\,, \tag{34}$$

and

$$\hat{\Lambda}_2(\hat{\mathbf{r}},\mathbf{d},\mathbf{e}) = 1 - \frac{\chi'}{2}\left(\frac{(\hat{\mathbf{r}}\cdot\mathbf{d}+\hat{\mathbf{r}}\cdot\mathbf{e})^2}{1+\chi'\mathbf{d}\cdot\mathbf{e}} + \frac{(\hat{\mathbf{r}}\cdot\mathbf{d}-\hat{\mathbf{r}}\cdot\mathbf{e})^2}{1-\chi'\mathbf{d}\cdot\mathbf{e}}\right). \tag{35}$$

The parameter χ in (34) is related to the anisotropy in the shape of the molecule, and is given in terms of the ratio $\varsigma = \sigma_e/\sigma_s$ of the length σ_e of the molecule to its breadth σ_s by

$$\chi = \frac{\varsigma^2 - 1}{\varsigma^2 + 1}\,. \tag{36}$$

In (35), χ' is given by

$$\chi' = \frac{(\varepsilon_e/\varepsilon_s)^{1/\mu} - 1}{(\varepsilon_e/\varepsilon_s)^{1/\mu} + 1}\,, \tag{37}$$

where $\varepsilon_e/\varepsilon_s$ denotes the ratio of the strength parameter for end-to-end configuration of the molecules to that parameter for side-to-side configuration. The strength parameter is chosen according to Berne and Pechukas [53]

to be of the form

$$\hat{\Gamma}(\mathbf{r},\mathbf{d},\mathbf{e}) = \exp\left(\frac{-|\mathbf{r}|^2}{\hat{\sigma}^2(\mathbf{r},\mathbf{d},\mathbf{e})}\right). \tag{38}$$

In (38), $\hat{\sigma}$ is called the range parameter and is given by

$$\hat{\sigma}(\hat{\mathbf{r}},\mathbf{d},\mathbf{e}) = \frac{\sigma_\circ}{\left[1-\frac{\chi}{2}\left(\frac{(\hat{\mathbf{r}}\cdot\mathbf{d}+\hat{\mathbf{r}}\cdot\mathbf{e})^2}{1+\chi\mathbf{d}\cdot\mathbf{e}}+\frac{(\hat{\mathbf{r}}\cdot\mathbf{d}-\hat{\mathbf{r}}\cdot\mathbf{e})^2}{1-\chi\mathbf{d}\cdot\mathbf{e}}\right)\right]^{1/2}}, \tag{39}$$

where

$$\sigma_\circ = \sqrt{2}\sigma_s. \tag{40}$$

The parameter $\mu = 2$ is chosen according to a widely used value [79]. Also, we choose $\lambda = -1$. It is necessary to mention that the magnitude of λ includes the influence of the relative orientation of the molecules on the strength of the interaction between them. The sign of λ shows the preferred relative configuration between the molecules. Here, a negative sign for which the side-to-side configuration is preferred is selected.

The specific choice of the distance parameter $\hat{\Gamma}$ in (38) results an interaction potential that does not have a certain cutoff distance after which the interaction between the molecules does not exist. However, since the potential decays exponentially as a function of the distance between the molecules, it is possible to define an effective cutoff distance after which the interactions may be neglected.

Assuming a constant molecular density, (32) can be used in (A.10) to yield the flexural and torsional rigidities in terms of the molecular distribution function f, the fitting parameter $\Lambda_\circ$, the length scale $\sigma_\circ$, and the dimensionless parameter $x = d/\sigma_\circ$. While doing so yields

$$k_c = \frac{f^2\sigma_\circ^3\Lambda_\circ}{24}\Bigg(12x\chi^2 e^{-x^2}\left(\frac{x^2}{3}-\frac{1}{2}\right)(I+J) + 3\sqrt{\pi}\,\mathrm{erf}(x)(\chi^2(I+J)+2I)\Bigg), \tag{41}$$

for flexural rigidity, the torsional rigidity becomes

$$k_t = 0. \tag{42}$$

In (41), erf denotes the error function, and I and J are given by the integral representations

$$I = \int_0^{2\pi}\int_0^{2\pi}\frac{1}{(1-\chi^2\cos^2(\theta-\eta))^{1/2}}\,\mathrm{d}\theta\,\mathrm{d}\eta,$$
$$J = \int_0^{2\pi}\int_0^{2\pi}\frac{\cos 2(\theta-\eta)}{(1-\chi^2\cos^2(\theta-\eta))^{1/2}}\,\mathrm{d}\theta\,\mathrm{d}\eta. \tag{43}$$

Moreover, the resulting value for $\psi_\circ$ is given by

$$\psi_\circ = 4\sqrt{\pi}f^2\sigma_\circ\Lambda_\circ\,\mathrm{erf}(x)I. \tag{44}$$

Here we choose a specific type of surfactant molecules as an example to determine the aspect ratio of the equivalent spheroid in fig. 9. To do so, one may employ the equality of the volumes of the surfactant molecule and the replacing spheroid, and the equality of their lengths. A single surfactant molecule can be envisioned as a cylinder representing the tail, attached to a small sphere which represents the head [56]. Here we rely on the dimensions of a specific surfactant molecule cetyltrimethylammonium salicylate (CTA Sal)/organic salt sodium salicylate (NaSal-Water system) reported by Shikata *et al.* [56]. According to their estimation, the length of the aforementioned surfactant molecule from the center of the head-group to the tail is $\sim 2\,\mathrm{nm}$, and the diameters of the head-group and tail are $\sim 0.85\,\mathrm{nm}$ and $\sim 0.5\,\mathrm{nm}$, respectively. The total volume of that molecule is thus the sum of the volume of the spherical head and that of the cylindrical tail. To obtain a spheroid of the same volume, and with the same length as the tail of the surfactant molecule, the aspect ratio ς in fig. 9 is about 5.

The schematic of the term $\psi_\circ/f^2\sigma_\circ\Lambda_\circ$ and flexural rigidity $k_c/f^2\sigma_\circ^3\Lambda_\circ$ with respect to the dimensionless cutoff distance $d/\sigma_\circ$ for different molecular aspect ratios ς in the range of 1–5 has been depicted in fig. 10. Figure 10 (left part) shows that $\psi_\circ$ approaches an asymptote as the effective dimensionless cutoff distance increases. The same behaviour is observed for the flexural rigidity k_c in fig. 10 (right part). As is evident from the results of fig. 10, by increasing the aspect ratio ς of the molecules from one (corresponding to spherical particles) to higher values (corresponding to spheroids), the flexural rigidity k_c increases. This finding can be justified as follows. When the aspect ratio of the molecules increases, a large number of molecules may aggregate in a specific part of the body of wormlike micelle. Hence, the material is expected to be more resistant to bending. On the other hand, adjacent spherical molecules can easily roll on each other, and thus, the local resistance to bending of the structure made by such molecules is far less than that of the structure made by spheroidal particles.

According to fig. 10, there is negligible change in both $\psi_\circ$ and the flexural rigidity k_c for $d/\sigma_\circ > 4$. Thus, it is reasonable to consider the effective cutoff distance d to be $\sim 4\sigma_\circ$.

5.2 Persistence length of a wormlike micelle

For a wormlike micelle, persistence length ℓ_p is a characteristic length scale which gives an estimate of how flexible the micelle is [80]. This length scale can be measured using light or neutron scattering or flow birefringence techniques [34, 56]. A wormlike micelle usually has a characteristic persistence length between 10 to 150 nanometers [34, 81]. The persistence length ℓ_p of a wormlike micelle is given in terms of its flexural rigidity k_c by [82]

$$\ell_p = \frac{k_c}{2k_BT}. \tag{45}$$

By taking the effective dimensionless cutoff distance $x = d/\sigma_\circ$ as 4 according to fig. 10, (41) and (45) give

$$\ell_p = \frac{f^2\sigma_\circ^3\Lambda_\circ}{k_BT}\Bigg\{\frac{\sqrt{\pi}}{8}(2I+\chi^2(I+J))\,\mathrm{erf}(4) + \frac{29\,e^{-16}}{3}(I+J)\Bigg\}. \tag{46}$$

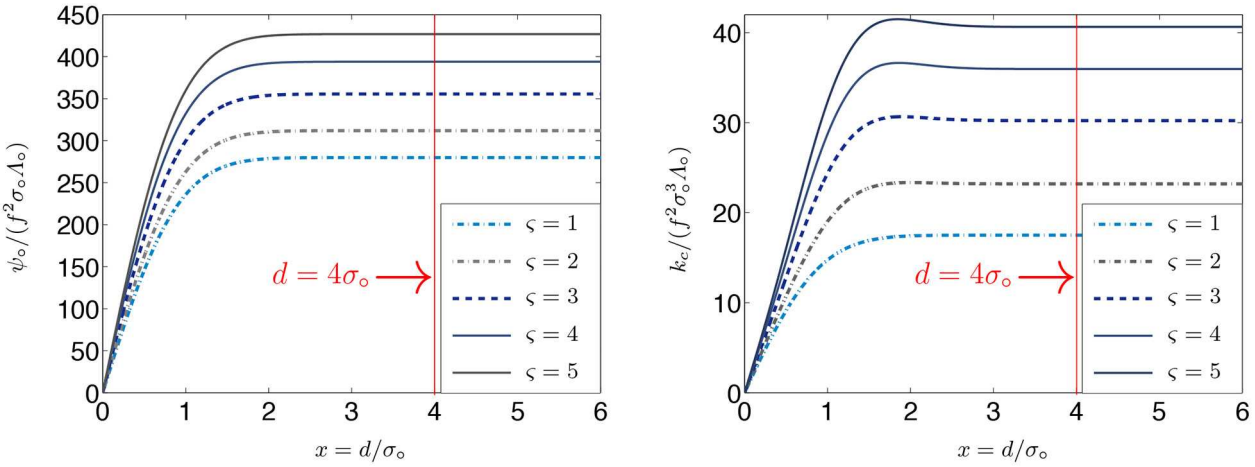

Fig. 10. Graph of the dimensionless parameter $\psi_\circ/(f^2\sigma_\circ\Lambda_\circ)$, and the dimensionless flexural rigidity $k_c/(f^2\sigma_\circ^3\Lambda_\circ)$ with respect to the ratio $d/\sigma_\circ$, as a consequence of applying modified Berne-Pechukas interaction potential, for different values of the aspect ratio $\varsigma = \sigma_e/\sigma_s$. As is evident from the plots, negligible change in $\psi_\circ/(f^2\sigma_\circ\Lambda_\circ)$ and $k_c/(f^2\sigma_\circ^3\Lambda_\circ)$ is observed after $d = 4\sigma_\circ$. Consequently, the effective cutoff distance after which the potential decays rapidly, can be reasonably approximated by $d = 4\sigma_\circ$.

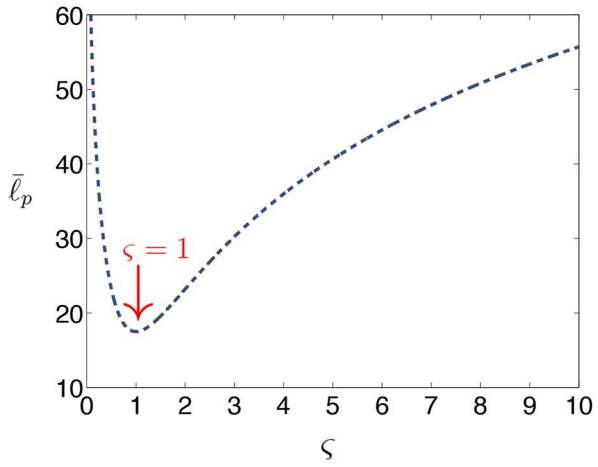

Fig. 11. Graph of the dimensionless persistence length $\bar{\ell}_p$ *versus* the molecular aspect ratio $\varsigma = \sigma_e/\sigma_s$.

The plot of the dimensionless persistence length

$$\bar{\ell}_p = \frac{k_B T \ell_p}{f^2\sigma_\circ^3\Lambda_\circ} \tag{47}$$

with respect to the molecular aspect ratio ς is depicted in fig. 11. As fig. 11 indicates, the minimum persistence length occurs when the aspect ratio ς approaches one, or equivalently, when the spheroidal particles become spherical ones. By increasing the aspect ratio the stiffness increases and as a result, ℓ_p increases. This finding is in agreement with the previous observation by Lauw *et al.* [40] They reported that the persistence length ℓ_p of a wormlike micelle has direct dependence upon the length of its constituent surfactant molecules.

5.3 Spherocylindrical-particle potential

Lintuvuori and Wilson [55] presented an anisotropic soft-core potential to describe the interaction between two rodlike molecules. The rodlike molecule in their model is replaced by a spherocylinder, as depicted schematically in fig. 12. In this potential, the interaction energy between two spherocylinders with intermolecular vector $\mathbf{r}$ and orientations $\mathbf{d}$ and $\mathbf{e}$ is given by

$$\hat{\Omega}(\mathbf{r},\mathbf{d},\mathbf{e}) = \begin{cases} \mathcal{F}(\mathbf{r},\mathbf{d},\mathbf{e}) & \text{if } |\mathbf{r}| < \sigma_\circ, \\ \mathcal{G}(\mathbf{r},\mathbf{d},\mathbf{e}) & \text{if } \sigma_\circ \le |\mathbf{r}| \le d^*(\hat{\mathbf{r}},\mathbf{d},\mathbf{e}), \\ 0 & \text{if } d^*(\hat{\mathbf{r}},\mathbf{d},\mathbf{e}) < |\mathbf{r}|, \end{cases} \tag{48}$$

where $\sigma_\circ$ denotes the breadth of the spherocylinder, and the parameter d^* is the distance between two spherocylinders after which the potential becomes zero; d^* depends on the orientation of the molecules and the unit vector $\hat{\mathbf{r}}$ associated with the intermolecular vector $\mathbf{r}$ in the form

$$d^*(\hat{\mathbf{r}},\mathbf{d},\mathbf{e}) = \sigma_\circ \left\{ 1 + \left(\frac{\Pi_1}{2\Pi_2 - 2\Phi(\hat{\mathbf{r}},\mathbf{d},\mathbf{e})} \right)^{1/2} \right\}. \tag{49}$$

In (48), $\mathcal{F}$ and $\mathcal{G}$ are given by

$$\begin{aligned} \mathcal{F}(\mathbf{r},\mathbf{d},\mathbf{e}) &= \Pi_1\Lambda_\circ \left(1 - \frac{|\mathbf{r}|}{\sigma_\circ}\right)^2 - \frac{\Pi_1^2\Lambda_\circ}{4(\Pi_2 - \Phi(\hat{\mathbf{r}},\mathbf{d},\mathbf{e}))}, \\ \mathcal{G}(\mathbf{r},\mathbf{d},\mathbf{e}) &= \Pi_1\Lambda_\circ \left(1 - \frac{|\mathbf{r}|}{\sigma_\circ}\right)^2 - \frac{\Pi_1^2\Lambda_\circ}{4(\Pi_2 - \Phi(\hat{\mathbf{r}},\mathbf{d},\mathbf{e}))} \\ &\quad - (\Pi_2 - \Phi(\hat{\mathbf{r}},\mathbf{d},\mathbf{e})) \left(1 - \frac{|\mathbf{r}|}{\sigma_\circ}\right)^4. \end{aligned} \tag{50}$$

Here, $\Lambda_\circ$ is a fitting parameter with the dimension of energy associated with the potential, and

$$\Phi(\hat{\mathbf{r}},\mathbf{d},\mathbf{e}) = 5\eta_1 P_2(\mathbf{d}\cdot\mathbf{e}) + 5\eta_2 (P_2(\hat{\mathbf{r}}\cdot\mathbf{d}) + P_2(\hat{\mathbf{r}}\cdot\mathbf{e})), \tag{51}$$

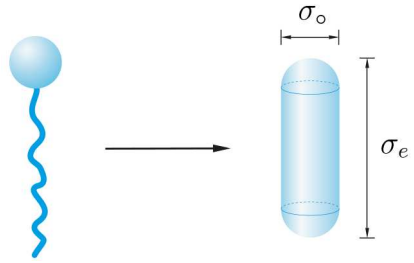

Fig. 12. Schematic of an equivalent spherocylinder for a surfactant molecule.

where $P_2(x) = (3x^2 - 1)/2$ is the second-order Legendre polynomial. Also, Π_1 and Π_2 in (50) and η_1 and η_2 in (51) are dimensionless parameters that specify the type of molecules under consideration.

Granted the equality of the volumes for the surfactant molecule and the spherocylinder, and also, the equality of the length of the tail and that of the spherocylinder depicted in fig. 12, and using the same reported dimensions of the surfactant molecule in the previous section, the aspect ratio $\sigma_e/\sigma_\circ$ of the spherocylinder is obtained within the range of $\sim$ 2–3. We choose $\Pi_1 = 70$, $\Pi_2 = 1500$, $\eta_1 = 120$, and $\eta_2 = -120$, which arise from molecular dynamics simulations of spherocylinders with preferred side-to-side configurations and aspect ratio $\sigma_e/\sigma_\circ = 3$ [55].

The cutoff distance d beyond which the interaction is negligible, can be determined by d^* in (49). In particular, d in our model is given by the maximal value of d^* ranging over all possible choices of $\hat{\mathbf{r}}$, $\mathbf{d}$, and $\mathbf{e}$. This maximal value is

$$d = \sigma_\circ \left\{ 1 + \left(\frac{\Pi_1}{2\Pi_2 - 10(\eta_1 - \eta_2)} \right)^{1/2} \right\} \approx 1.34\sigma_\circ. \quad (52)$$

As an approximation, we consider

$$d \approx 2\sigma_\circ. \quad (53)$$

Applying (48) to the present model in (A.10) gives the value of the line tension $\psi_\circ$ as

$$\psi_\circ = -826.7\pi^2 f^2 \Lambda_\circ \sigma_\circ, \quad (54)$$

and the values of the flexural and torsional rigidities as

$$k_c = 1178\pi^2 f^2 \Lambda_\circ \sigma_\circ^3, \qquad \text{and} \qquad k_t = 0. \quad (55)$$

Hence, the persistence length ℓ_p reads

$$\ell_p = 589\pi^2 \frac{f^2 \Lambda_\circ \sigma_\circ^3}{k_B T}. \quad (56)$$

The fitting parameter $\Lambda_\circ$ associated with each of the anisotropic interaction potentials in (46) or (56) may be selected in a way that the resulting value for persistence length is consistent with those obtained through experiments and numerical simulations. Notice that the fitting parameter $\Lambda_\circ$ in (46) is not the same as the one in (56), since it is associated with a different interaction potential.

The flexural and torsional rigidities k_c and k_t control the sensitivity of the derived free-energy density (20) to changes of the curvature κ and torsion τ of the centerline $\mathcal{C}$ of the wormlike micelle. Application of the two soft-core interaction potentials on our model yield zero values for torsional rigidity k_t. This outcome might imply that the term including the torsion τ in the free-energy density (20) is less significant than the other two terms. As a consequence, it might be reasonable to consider the first two terms in the right-hand side of (20) as the elastic free energy of the wormlike micelle, unless the torsion τ of the curve $\mathcal{C}$ at a given point takes a very large value.

Notice that the flexural rigidity k_c in Canham-Helfrich free-energy density (1) has the dimension of energy, and thus, using that term in (45) yields a dimensionless value for the persistence length ℓ_p of the wormlike micelle. However, using the flexural rigidity k_c in the free-energy density (20), which has the dimension of energy times length, results the persistence length ℓ_p with the dimension of length.

6 Application of the model on toroidal micelles and comparison with previous studies

In this section, we expand the result of sect. 4.2 by employing necessary statistical and thermodynamical concepts [1, 2, 42, 83], to make a comparison between the results of our model and the previous studies.

On thermodynamical grounds, the total free energy E_{tot} of the process of self-assembly of N surfactant molecules into a single toroidal micelle can be considered as the sum of two terms: the interaction free energy of forming a toroidal micelle out of N surfactant molecules, which we denote by $N\psi_{\text{mic}}$, and the unfavourable free energy ΔG_{tor} of self-assembling surfactants, which is the positive expression $\Delta G_{\text{tor}} = -T\Delta S_{\text{tor}}$ [83]. It follows from the set of thermodynamics equilibrium conditions [42]

$$\Delta G_{\text{tot}} = N\psi_{\text{mic}} + \Delta G_{\text{tor}} = 0, \quad (57)$$

that ψ_{mic} should be a negative quantity in order for the process to be thermodynamically feasible. The ideal entropy S_{free} of mixing N surfactant molecules with N_s solvent molecules is

$$S_{\text{free}} = -k_B \left(N \ln \phi_{\text{free}} + N_s \ln \phi_s \right), \quad (58)$$

where ϕ_s and ϕ_{free} are the volume fractions of the solvent and surfactants, respectively. Similarly, the entropy S_{tor} of the mixture of a single toroidal micelle in N_s solvent molecules is

$$S_{\text{tor}} = -k_B \left(\ln \phi_N + N_s \ln \phi_s \right), \quad (59)$$

where ϕ_N is the volume fraction of a single toroidal micelle [83]. Considering (58) and (59), one can simply obtain the entropy change ΔS_{tor} corresponding to the self-assembly of N surfactant molecules to a single toroidal micelle as

$$\Delta S_{\text{tor}} = S_{\text{tor}} - S_{\text{free}} = -k_B \left(\ln \phi_N - N \ln \phi_{\text{free}} \right). \quad (60)$$

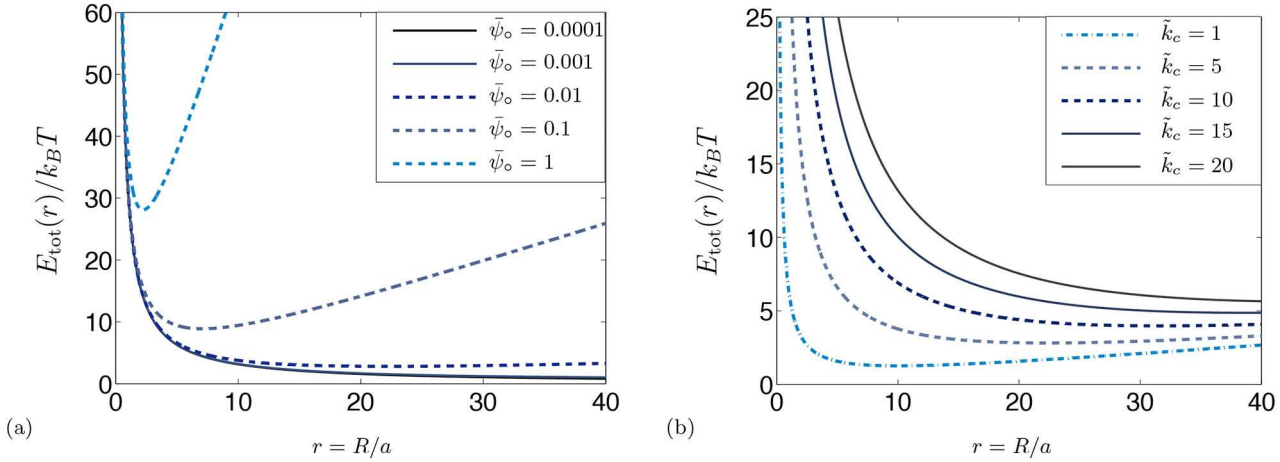

Fig. 13. Schematic of the dimensionless net free energy of a toroidal micelle against the dimensionless radius r of the torus, based on our theory. (a) The value of the flexural rigidity was set to $k_c/a = 5\,k_BT$ [42], and some arbitrary values for $\bar{\psi}_\circ = a\psi_\circ/k_BT$ were selected. (b) The parameter $\bar{\psi}_\circ$ was set to 1, and the value of $\tilde{k}_c = k_c/(a\,k_BT)$ was selected in the range 1–20. The convexity of energy plots indicates the stability of the corresponding equilibrium state. Similar to the previous reports [41], positiveness of the flexural rigidity is a necessary condition for stability.

In view of (60) and

$$\Delta G_{\rm tor} = -T\Delta S_{\rm tor} = k_BT\left(\ln\phi_N - N\ln\phi_{\rm free}\right), \qquad (61)$$

the right-hand side equality in (57) simplifies to

$$N\psi_{\rm mic} + k_BT\left(\ln\phi_N - N\ln\phi_{\rm free}\right) = 0. \qquad (62)$$

On introducing the free energy $E_{\rm tot}$ of the formation of a toroidal micelle out of N surfactant molecules (excluding the translational entropy) as [1]

$$E_{\rm tot} := N\psi_{\rm mic} - Nk_BT\ln\phi_{\rm free}, \qquad (63)$$

(62) can be expressed alternatively as

$$E_{\rm tot} + k_BT\ln\phi_N = 0. \qquad (64)$$

Straightforward calculation based on (64) leads to

$$\phi_N = \exp\left(\frac{-E_{\rm tot}}{k_BT}\right). \qquad (65)$$

Notice that the volume fraction density ϕ_N of a specific aggregate comprised of N surfactant monomers in a micellar solution can be alternatively obtained by minimizing the Flory-Huggins [84–86] free-energy functional for a binary mixture, written in terms of the densities of the different species, and Lagrange multipliers fixing the total surfactant density. The total volume fraction $\varphi_{\rm tot}$ may be expressed as the summation of the size distribution function [83]

$$\varphi_{\rm tot} = \sum_1^\infty \phi_N, \qquad (66)$$

which, according to Bergström [83], can be approximated by

$$\int_1^\infty \frac{{\rm d}N}{{\rm d}r}\exp\left(\frac{-E_{\rm tot}(r)}{k_BT}\right){\rm d}r. \qquad (67)$$

In (67), r denotes the ratio of the major radius R of the torus, to its minor radius ξ (see fig. 6). Following Bergström [42], the total volume fraction density $\Phi_{\rm tot}$ is the integrand of the right-hand side of (67). Hence, the total volume fraction density (or the size distribution function) $\Phi_{\rm tot}$ of a toroidal micelle comprised of N surfactant molecules is given in terms of its net free energy $E_{\rm tot}(r)$ by

$$\Phi_{\rm tot} = \frac{{\rm d}N}{{\rm d}r}\exp\left(\frac{-E_{\rm tot}(r)}{k_BT}\right). \qquad (68)$$

The quantity N can be obtained by equating the volume of the tails of N surfactant molecules comprising the micelle, and that occupied by the toroidal micelle [42]. On representing the volume of the tail of a single surfactant molecule by v, the volume of N surfactant molecules forming the toroidal micelle is Nv. On the other hand, the volume of a torus with the minor radius ξ and major radius R can be obtained by applying the second Pappus-Guldinus theorem [87]. Hence,

$$Nv = (2\pi)(\pi a^2)R = 2\pi^2a^3r, \qquad (69)$$

which results

$$\frac{dN}{dr} = \frac{2\pi^2a^3}{v}. \qquad (70)$$

Consequently, (68) becomes

$$\Phi_{\rm tot} = \frac{2\pi^2a^3r}{v}\exp\left(\frac{-E_{\rm tot}(r)}{k_BT}\right). \qquad (71)$$

According to $r = R/a$, the net free energy $E_{\rm tot}$ of a toroidal micelle in (26) takes the form

$$E_{\rm tot}(r) = 2\pi ar\left(\psi_\circ + \frac{k_c}{r^2a^2}\right), \qquad (72)$$

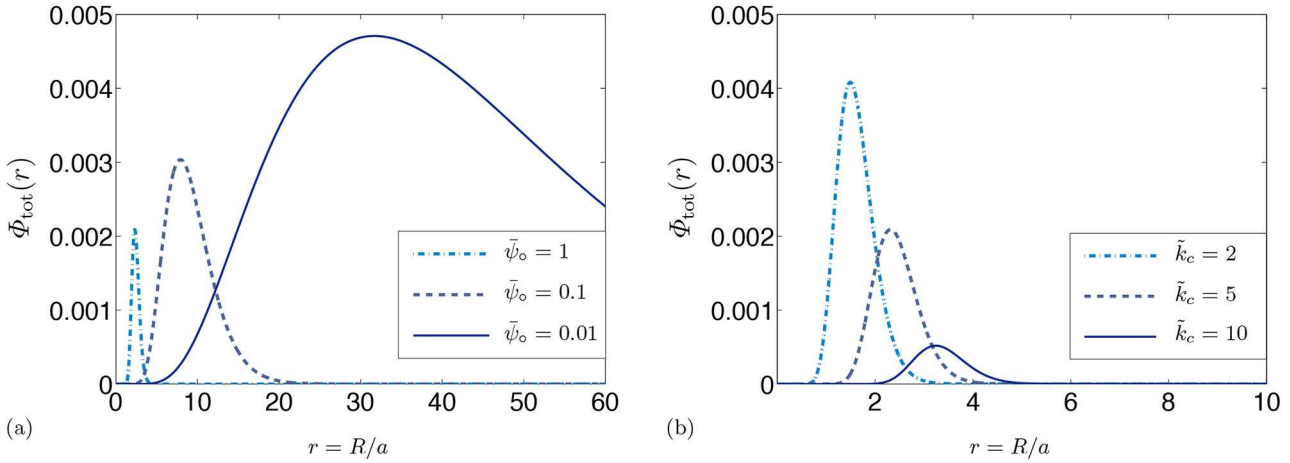

Fig. 14. Schematic of the volume fraction density $\Phi_{\rm tot}$ of toroidal micelles in terms of $r = R/a$, based on our model. Arbitrary factors have been used to make each set of the plots in a single frame. (a) The value of the flexural rigidity was set to $k_c/a = 5\,k_BT$ [42] and the parameter $\bar{\psi}_\circ = a\psi_\circ/k_BT$ was selected in the range 0.01–1. (b) The value of $\bar{\psi}_\circ$ was set to 1, and the flexural rigidity $\tilde{k}_c = k_c/(a\,k_BT)$ was selected in the range 2–10.

or, equivalently, the dimensionless form

$$\frac{E_{\rm tot}(r)}{k_BT} = \frac{2\pi r}{k_BT}\left(a\psi_\circ + \frac{k_c/a}{r^2}\right). \tag{73}$$

Figure 13 displays the dimensionless free energy $E_{\rm tot}/k_BT$ of a toroidal micelle against the ratio r. Granted that $\psi_\circ$ and k_c remain positive, the net free energy $E_{\rm tot}$ is convex and possesses a minimum point corresponding to the stable equilibrium state. Further, the range of the obtained values of the minimum free energy of a toroidal micelle in fig. 13 is on the same order of magnitude with that obtained by Bergström [42].

Applying (73) in (71) results the final form of the volume fraction density $\Phi_{\rm tot}$. The schematic of $\Phi_{\rm tot}$ for a set of previously reported values of the flexural rigidity k_c, and some arbitrary values of the parameter $\psi_\circ$ is depicted in fig. 14. As fig. 14b indicates, size distribution function of toroidal micelles decreases by increasing the value of the flexural rigidity k_c, which is consistent with the previous findings [42]. The histogram of experimental data can be fitted to the theoretical size distribution function $\Phi_{\rm tot}$ in (71) to find the real values of the material properties k_c and $\psi_\circ$. Recall that the size distribution function $\Phi_{\rm tot}$ is a function of the total free energy $E_{\rm tot}$, which depends on $\psi_\circ$ and k_c of the toroidal micelle. To simplify yet provide physically meaningful curve fit, by fixing the value of flexural rigidity k_c, one can obtain the corresponding best values of $\psi_\circ$ by fitting the size distribution function $\Phi_{\rm tot}$ over the histogram of the experimental data. Specifically, one can rely on a range of representative values for the flexural rigidity of wormlike micelles reported in previous studies. For instance, Jung *et al.* [88] reported the flexural rigidity in the range of 1–8k_BT for cetyltrimethylammonium bromide (CTAB)-based aggregates. More specifically, Bergström [42] set the flexural rigidity of a single toroidal micelle made of ionic surfactants to be 1–5k_BT. Based on these literature reports, one may select the value of flexural rigidity for a toroidal micelle. Using such a range of representative values for the flexural rigidity, one can fit the theoretical size distribution $\Phi_{\rm tot}$ in (71) to the histogram of the experimental data to find the interval of values for $\psi_\circ$.

7 Conclusion

The extensive application of surfactants motivates comprehensive and predictive theoretical studies that improve our understanding of the behaviour of these complex systems. In the first part of the present study, an expression for the elastic free-energy density of a wormlike micelle was derived taking into account interactions between its constituent amphiphilic molecules. The resulting expression apply only to micelles that are sufficiently long in comparison to the length of a surfactant molecule. Such micelles are modeled as a tube with circular cross-section of constant diameter whose shape is characterized by their centerlines. The free-energy density of a wormlike micelle is found to incorporate the sum of a quadratic function of the curvature and a quadratic function of the torsion of its centerline. The structure of the derived free-energy density is similar to that of free-energy density functions of polymer chains and helical filaments such as DNA. In contrast to such models, the derived model does not exhibit intrinsic curvature nor intrinsic torsion. For a wormlike micelle consisting of more than one type of surfactant molecules, the presence of molecules with different head-group or tail conformations might lead to intrinsic curvature or intrinsic torsion. According to our modeling assumptions, such effects are ruled out.

Using the derived free-energy density, the net free energy of either closed or open wormlike micelles were derived. Whereas the total free energy of a closed wormlike micelle is obtained simply by integrating its free-energy

density over its centerline, the total free energy of an open wormlike micelle includes two additional contributions from its end caps.

The derived model was applied on a special case of open wormlike micelles whose centerline has the shape of a circular arc. The model was also applied on a wormlike micelle of toroidal geometry. In both cases the minimum point corresponding to the equilibrium state was observed. The conditions under which linear chains in dilute systems transform into closed toroidal rings were further analyzed and discussed. It was concluded that in the dilute limit, shorter micellar chains are expected to be linear, and longer ones are expected to be closed rings.

The flexural and torsional rigidities k_c and k_t control the sensitivity of the derived free-energy density (20) to changes of the curvature and torsion of the centerline of the wormlike micelle. The derivation of the model gives rise to integral representations for the flexural and torsional rigidities that involve a generic interaction potential. Two concrete soft-core interaction potentials, one without a specific cutoff distance for spheroidal molecules, and the other with a defined cutoff distance for spherocylindrical molecules, are considered. The integrals representing the moduli are evaluated to yield explicit expressions for flexural and torsional rigidities in terms of the molecular distribution function, molecular dimensions, cutoff distance, and the fitting parameter associated with the potentials. The interaction potentials yield zero torsional rigidity, and nonzero flexural rigidity. This outcome transpires that the term corresponding torsion in the derived free energy has less significance than the effect of curvature. The persistence length of a wormlike micelle was found based on the results coming from the application of the interaction potentials. The results show that wormlike micelles with longer surfactant molecules have higher persistence length which is in accord with the previous observations. The fitting parameter associated with each anisotropic interaction potential can be selected in a way that the resulting value for persistence length takes the reported values obtained through experiments.

Finally, the developed model was applied to toroidal wormlike micelles, and the results were compared with those found in the literature. The range of the minimum free energy of a toroidal micelle was found to be on the same order of magnitude as the predictions previously reported. Further, our theory predicted that the equilibrium state of toroidal micelles is stable for positive values of flexural rigidity, which is analogous to the prior predictions. Applying statistical-thermodynamical concepts following previous studies, the theoretical size distribution of a toroidal micelle was found in terms of the derived free energy. Consistent with the previous observations, it was found that the size distribution of the toroidal micelle decreases by increasing the value of its flexural rigidity. Fitting the theoretical size distribution to the experimental data, the intervals of values for material parameters can be found.

Financial support from NIH (NIDCD) grant DC 005788 is gratefully acknowledged. The author thanks the anonymous reviewer for very helpful and constructive comments, Brian Seguin for fruitful discussions, Mohsen Maleki for figs. 1–6, and Prof. Norman Wagner for the introduction of useful references.

Appendix A.

In this section, the details of the expansion of the right-hand side of (19) is carried out. On performing the change of variables $t - t_\circ = \delta s$ and defining $\bar{\mathbf{r}}(s) = \mathbf{x}(t_\circ) - \mathbf{x}(t_\circ + \delta s)$, (19) becomes

$$\psi = \delta \int_{-t_\circ/\delta}^{(L-t_\circ)/\delta} \int_0^{2\pi} \int_0^{2\pi} \hat{\Omega}\Big(\frac{|\bar{\mathbf{r}}(s)|^2}{\delta^2}, \bar{\mathbf{r}}(s)\cdot\mathbf{d}(t_\circ,\theta), \bar{\mathbf{r}}(s)\cdot\mathbf{e}(t_\circ+\delta s,\eta), \mathbf{d}(t_\circ,\theta)\cdot\mathbf{e}(t_\circ+\delta s,\eta)\Big) \times f(t_\circ) f(t_\circ+\delta s)\,\mathrm{d}\theta\,\mathrm{d}\eta\,\mathrm{d}s. \tag{A.1}$$

We wish to expand the right-hand side of (A.1) in powers of δ neglecting terms of $o(\delta^2)$. The following abbreviations are used:

$$\left.\begin{aligned} &\mathbf{n} := \mathbf{n}(t_\circ), \quad \mathbf{t} := \mathbf{t}(t_\circ), \quad \mathbf{b} := \mathbf{b}(t_\circ), \\ &f := f(t_\circ), \quad f' := f'(t_\circ), \quad f'' := f''(t_\circ). \end{aligned}\right\} \tag{A.2}$$

To achieve the expansion of the right-hand side of (A.1), the following expansions are used:

$$\begin{aligned} \mathbf{x}(t_\circ+s\delta) &= \mathbf{x}(t_\circ) + \left(\frac{s^2\delta^2}{2}\kappa + \frac{s^3\delta^3}{6}\kappa'\right)\mathbf{n} + \left(\frac{s^3\delta^3}{6}\kappa\tau\right)\mathbf{b} \\ &\quad + \left(s\delta - \frac{s^3\delta^3}{6}\kappa^2\right)\mathbf{t} + o(\delta^3), \\ \mathbf{n}(t_\circ+s\delta) &= \left(1 - \frac{s^2\delta^2}{2}(\kappa^2+\tau^2)\right)\mathbf{n} + \left(s\delta\tau + \frac{s^2\delta^2}{2}\tau'\right)\mathbf{b} \\ &\quad - \left(s\delta\kappa + \frac{s^2\delta^2}{2}\kappa'\right)\mathbf{t} + o(\delta^2), \\ \mathbf{b}(t_\circ+s\delta) &= -\left(s\delta\tau + \frac{s^2\delta^2}{2}\tau'\right)\mathbf{n} + \left(1 - \frac{s^2\delta^2}{2}\tau^2\right)\mathbf{b} \\ &\quad + \left(\frac{s^2\delta^2}{2}\kappa\tau\right)\mathbf{t} + o(\delta^2), \\ f(t_\circ+s\delta) &= f + s\delta f' + \left(\frac{s^2\delta^2}{2}\right)f'' + o(\delta^2). \end{aligned} \tag{A.3}$$

By neglecting the higher-order terms and performing the dot products, the arguments of $\hat{\Omega}$ in the right-hand side of eq. (A.1) become

$$\begin{aligned} &\frac{|\mathbf{x}(t_\circ) - \mathbf{x}(t_\circ+s\delta)|^2}{\delta^2} = s^2 + A_1\delta^2 s^4 + o(\delta^2), \\ &(\mathbf{x}(t_\circ) - \mathbf{x}(t_\circ+s\delta))\cdot\mathbf{d}(t_\circ,\theta) = A_2\delta^2 s^2 + o(\delta^2), \\ &(\mathbf{x}(t_\circ) - \mathbf{x}(t_\circ+s\delta))\cdot\mathbf{e}(t_\circ+s\delta,\eta) = A_3\delta^2 s^2 + o(\delta^2), \\ &\mathbf{d}(t_\circ,\theta)\cdot\mathbf{e}(t_\circ+s\delta,\eta) = A + A_4\delta s + A_5\delta^2 s^2 + o(\delta^2), \end{aligned} \tag{A.4}$$

where the coefficients A_1–A_5 in (A.4) are expressed as

$$A = \cos(\theta-\eta), \qquad A_1 = -\frac{1}{12}\kappa^2, \qquad A_2 = -\frac{1}{2}\kappa\cos\theta,$$
$$A_3 = \frac{1}{2}\kappa\cos\eta, \qquad A_4 = \tau\sin(\theta-\eta),$$
$$A_5 = \frac{1}{2}\left(\tau'\sin(\theta-\eta) - \kappa^2\cos\theta\cos\eta - \tau^2\cos(\theta-\eta)\right). \tag{A.5}$$

The identities

$$\mathbf{t}' = \kappa\mathbf{n}, \qquad \mathbf{n}' = -\kappa\mathbf{t} + \tau\mathbf{b}, \qquad \mathbf{b}' = -\tau\mathbf{n}, \tag{A.6}$$

called the Frenet-Serret formulas [89], which express the derivatives of $\mathbf{t}$, $\mathbf{n}$, and $\mathbf{b}$ with respect to the arclength s in terms of the Frenet frame $\{\mathbf{t},\mathbf{n},\mathbf{b}\}$ of $\mathcal{C}$ are used in (A.3). It should be noted that although the quantities A_1 through A_5 depend on θ and η, this dependence will not be denoted explicitly. Finally, put

$$\bar{\Omega}(s,\theta,\eta) := \hat{\Omega}(s^2,0,0,\cos(\theta-\eta)),$$
$$\bar{\Omega}_{,i}(s,\theta,\eta) := \hat{\Omega}_{,i}(s^2,0,0,\cos(\theta-\eta)),$$
$$\bar{\Omega}_{,ii}(s,\theta,\eta) := \hat{\Omega}_{,ii}(s^2,0,0,\cos(\theta-\eta)),$$
$$i \in \{1,2,3,4\}. \tag{A.7}$$

Using the expansions (A.4) and the abbreviations (A.7), while knowing $\frac{-t_\circ}{\delta} \ll -\ell$ and $\ell \ll \frac{L-t_\circ}{\delta}$ and using (16), the right-hand side of (A.1) is, on neglecting terms proportional to δ^3 and higher,

$$\begin{aligned}\psi = {} & \delta\int_{-\ell}^{\ell}\int_0^{2\pi}\int_0^{2\pi}\bar{\Omega}(s,\theta,\eta)f^2\,\mathrm{d}\theta\,\mathrm{d}\eta\,\mathrm{d}s \\ & + \delta^3\int_{-\ell}^{\ell}\int_0^{2\pi}\int_0^{2\pi}\frac{1}{2}\bar{\Omega}(s,\theta,\eta)ff''s^2\,\mathrm{d}\theta\,\mathrm{d}\eta\,\mathrm{d}s \\ & + \kappa^2\Big\{\delta^3\int_{-\ell}^{\ell}\int_0^{2\pi}\int_0^{2\pi} -\frac{f^2s^2}{12}\big[6\,\cos\theta\cos\eta\,\bar{\Omega}_4(s,\theta,\eta) \\ & + \bar{\Omega}_1(s,\theta,\eta)s^2\big]\,\mathrm{d}\theta\,\mathrm{d}\eta\,\mathrm{d}s\Big\} \\ & + \tau^2\Big\{\delta^3\int_{-\ell}^{\ell}\int_0^{2\pi}\int_0^{2\pi}\frac{f^2s^2}{2}\big[\sin^2(\theta-\eta)\bar{\Omega}_{44}(s,\theta,\eta) \\ & - \cos(\theta-\eta)\,\bar{\Omega}_4(s,\theta,\eta)\big]\mathrm{d}\theta\,\mathrm{d}\eta\,\mathrm{d}s\Big\},\end{aligned} \tag{A.8}$$

which is the free-energy density in terms of the curvature and torsion. The final form of the free-energy density for a wormlike micelle is thus of the form

$$\psi = \psi_\circ + k_c\kappa^2 + k_t\tau^2, \tag{A.9}$$

where

$$\begin{aligned}\psi_\circ = {} & \delta\int_{-\ell}^{\ell}\int_0^{2\pi}\int_0^{2\pi}\bar{\Omega}(s,\theta,\eta)f^2\,\mathrm{d}\theta\,\mathrm{d}\eta\,\mathrm{d}s \\ & + \delta^3\int_{-\ell}^{\ell}\int_0^{2\pi}\int_0^{2\pi}\frac{1}{2}\bar{\Omega}(s,\theta,\eta)ff''s^2\,\mathrm{d}\theta\,\mathrm{d}\eta\,\mathrm{d}s, \\ k_c = {} & \delta^3\int_{-\ell}^{\ell}\int_0^{2\pi}\int_0^{2\pi} -\frac{f^2s^2}{12}\big(6\,\cos\theta\cos\eta\,\bar{\Omega}_4(s,\theta,\eta) \\ & + \bar{\Omega}_1(s,\theta,\eta)s^2\big)\,\mathrm{d}\theta\,\mathrm{d}\eta\,\mathrm{d}s, \\ k_t = {} & \delta^3\int_{-\ell}^{\ell}\int_0^{2\pi}\int_0^{2\pi}\frac{f^2s^2}{2}\big(\sin^2(\theta-\eta)\bar{\Omega}_{44}(s,\theta,\eta) \\ & - \cos(\theta-\eta)\,\bar{\Omega}_4(s,\theta,\eta)\big)\mathrm{d}\theta\,\mathrm{d}\eta\,\mathrm{d}s.\end{aligned} \tag{A.10}$$

References

1. J.N. Israelachvili, *Intermolecular and Surface Forces: Revised Third Edition* (Academic press, 2011).
2. J.N. Israelachvili, D.J. Mitchell, B.W. Ninham, J. Chem. Soc. Faraday Trans. 2 **72**, 1525 (1976).
3. M. Cates, S. Candau, J. Phys.: Condens. Matter **2**, 6869 (1990).
4. B.M. Discher, Y.-Y. Won, D.S. Ege, J.C. Lee, F.S. Bates, D.E. Discher, D.A. Hammer, Science **284**, 1143 (1999).
5. H. Cui, Z. Chen, S. Zhong, K.L. Wooley, D.J. Pochan, Science **317**, 647 (2007).
6. A. Bernheim-Groswasser, R. Zana, Y. Talmon, J. Phys. Chem. B **104**, 4005 (2000).
7. G. Porte, R. Gomati, O. El Haitamy, J. Phys. Chem. **90**, 5746 (1986).
8. R. Zana, E.W. Kaler, *Giant Micelles: Properties and Applications* (CRC Press, 2007).
9. L. van Dam, G. Karlsson, K. Edwards, Biochim. Biophys. Acta **1664**, 241 (2004).
10. C. Oelschlaeger, M. Schopferer, F. Scheffold, N. Willenbacher, Langmuir **25**, 716 (2008).
11. E. Boek, J. Padding, V. Anderson, W. Briels, J. Crawshaw, J. Non-Newton. Fluid Mech. **146**, 11 (2007).
12. S. Lerouge, J.-F. Berret, Adv. Polym. Sci. **230**, 1 (2010).
13. N. Spenley, M. Cates, T. McLeish, Phys. Rev. Lett. **71**, 939 (1993).
14. Y.-Y. Won, H.T. Davis, F.S. Bates, Science **283**, 960 (1999).
15. C.A. Dreiss, Soft Matter **3**, 956 (2007).
16. J. Yang, Curr. Opin. Colloid Interface Sci. **7**, 276 (2002).
17. S. Komura, S. Safran, Eur. Phys. J. E **5**, 337 (2001).
18. S. Ezrahi, E. Tuval, A. Aserin, Adv. Colloid Interface Sci. **128**, 77 (2006).
19. A. Trent, R. Marullo, B. Lin, M. Black, M. Tirrell, Soft Matter **7**, 9572 (2011).
20. M. Black, A. Trent, Y. Kostenko, J.S. Lee, C. Olive, M. Tirrell, Adv. Mater. **24**, 3845 (2012).
21. M. Yang, D. Xu, L. Jiang, L. Zhang, D. Dustin, R. Lund, L. Liu, H. Dong, Chem. Commun. **50**, 4827 (2014).
22. J. Padding, E. Boek, Europhys. Lett. **66**, 756 (2004).
23. J.-F. Berret, in *Molecular Gels*, edited by P. Terech, R. Weiss (Elsevier, New York, 2004).

24. E. Boek, J. Padding, W. den Otter, W. Briels, J. Phys. Chem. B **109**, 19851 (2005).
25. L. Zhou, G.H. McKinley, L.P. Cook, J. Non-Newton. Fluid Mech. **211**, 70 (2014).
26. N. Germann, L. Cook, A. Beris, J. Non-Newton. Fluid Mech. **196**, 51 (2013).
27. V. Andreev, A. Victorov, Mol. Phys. **105**, 239 (2007).
28. D.P. Acharya, H. Kunieda, J. Phys. Chem. B **107**, 10168 (2003).
29. D.P. Acharya, H. Kunieda, Adv. Colloid Interface Sci. **123**, 401 (2006).
30. S.R. Raghavan, G. Fritz, E.W. Kaler, Langmuir **18**, 3797 (2002).
31. K. Kuperkar, L. Abezgauz, D. Danino, G. Verma, P. Hassan, V. Aswal, D. Varade, P. Bahadur, J. Colloid Interface Sci. **323**, 403 (2008).
32. O. Radulescu, P. Olmsted, J. Decruppe, S. Lerouge, J.-F. Berret, G. Porte, Europhys. Lett. **62**, 230 (2003).
33. A. Khatory, F. Lequeux, F. Kern, S. Candau, Langmuir **9**, 1456 (1993).
34. F. Nettesheim, N.J. Wagner, Langmuir **23**, 5267 (2007).
35. B.A. Schubert, E.W. Kaler, N.J. Wagner, Langmuir **19**, 4079 (2003).
36. S. May, Y. Bohbot, A. Ben-Shaul, J. Phys. Chem. B **101**, 8648 (1997).
37. P.B. Canham, J. Theor. Biol. **26**, 61 (1970).
38. W. Helfrich, Z. Naturforsch. C Bio. Sci. **28**, 693 (1973).
39. M. Tang, W.C. Carter, J. Phys. Chem. B **117**, 2898 (2013).
40. Y. Lauw, F.A. Leermakers, J. Phys. Chem. B **107**, 10912 (2003).
41. L.M. Bergström, ChemPhysChem **8**, 462 (2007).
42. L.M. Bergström, J. Colloid Interface Sci. **327**, 191 (2008).
43. S. Puvvada, D. Blankschtein, J. Chem. Phys. **92**, 3710 (1990).
44. R. Nagarajan, E. Ruckenstein, Langmuir **7**, 2934 (1991).
45. L.M. Bergström, J. Colloid Interface Sci. **293**, 181 (2006).
46. J. Padding, E. Boek, Phys. Rev. E **70**, 031502 (2004).
47. Y. Roiter, S. Minko, J. Am. Chem. Soc. **127**, 15688 (2005).
48. O. Kratky, G. Porod, Recl. Trav. Chim. Pays-Bas **68**, 1106 (1949).
49. P. Bugl, S. Fujita, J. Chem. Phys. **50**, 3137 (2003).
50. J.B. Keller, G.J. Merchant, J. Stat. Phys. **63**, 1039 (1991).
51. B. Seguin, E. Fried, J. Math. Biol. **68**, 647 (2014).
52. M. Asgari, A. Biria, Int. J. Nonlinear Mech. **76**, 135 (2015).
53. B.J. Berne, P. Pechukas, J. Chem. Phys. **56**, 4213 (2003).
54. J.G. Gay, B.J. Berne, J. Chem. Phys. **74**, 3316 (1981).
55. J.S. Lintuvuori, M.R. Wilson, J. Chem. Phys. **128**, 044906 (2008).
56. T. Shikata, S.J. Dahman, D.S. Pearson, Langmuir **10**, 3470 (1994).
57. S. Jain, F.S. Bates, Science **300**, 460 (2003).
58. T. Vermonden, J. van der Gucht, P. de Waard, A.T.M. Marcelis, N.A.M. Besseling, E.J.R Sudhölter, G.J. Fleer, M.A. Cohen Stuart, Macromolecules **36**, 7035 (2003).
59. C. Truesdell, W. Noll, *The Non-Linear Field Theories of Mechanics* (Springer, 2004).
60. P.G. de Prado Salas, M. Encinar, A. Alonso, M. Velez, P. Tarazona, Chem. Phys. Lipids **185**, 141 (2015).
61. L.M. Bergström, Langmuir **25**, 1949 (2009).
62. M. Gradzielski, Curr. Opin. Colloid Interface Sci. **8**, 337 (2003).
63. A. Goriely, P. Shipman, Phys. Rev. E **61**, 4508 (2000).
64. L. Landau, E. Lifshitz, *Elasticity Theory* (Pergamon Press, 1975).
65. Y. Liu, T. Pérez, W. Li, J. Gunton, A. Green, J. Chem. Phys. **134**, 065107 (2011).
66. J.F. Marko, E.D. Siggia, Macromolecules **27**, 981 (1994).
67. A. Balaeff, L. Mahadevan, K. Schulten, Phys. Rev. E **73**, 031919 (2006).
68. M.E. Cates, T.A. Witten, Macromolecules **19**, 732 (1986).
69. W.M. Gelbart, A. Ben-Shaul, J. Phys. Chem. **100**, 13169 (1996).
70. M. In, O. Aguerre-Chariol, R. Zana, J. Phys. Chem. B **103**, 7747 (1999).
71. S. May, Y. Bohbot, A. Ben-Shaul, J. Phys. Chem. B **105**, 630 (2001).
72. S.C. Sharma, L.K. Shrestha, K. Tsuchiya, K. Sakai, H. Sakai, M. Abe, J. Phys. Chem. B **113**, 3043 (2009).
73. S.A. Safran, L.A. Turkevich, Iampietro, P. Pincus, J. Phys. Lett. **45**, 69 (1984).
74. M.E. Cates, Macromolecules **20**, 2289 (1987).
75. S.J. Candau, F. Merikhi, G. Waton, P. Lemaréchal, J. Phys. **51**, 977 (1990).
76. P. Van Der Schoot, M.E. Cates, Europhys. Lett. **25**, 515 (1994).
77. G. Porte, J. Phys. Chem. **87**, 3541 (1983).
78. J.E. Jones, Proc. R. Soc. A **106**, 441 (1924).
79. L. Whitehead, C.M. Edge, J.W. Essex, J. Comput. Chem. **22**, 1622 (2001).
80. A. Ben-Shaul, D. Roux, *Micelles, Membranes, Microemulsions, and Monolayers* (Springer, Berlin, 1994).
81. M.R. Stukan, E.S. Boek, J.T. Padding, J.P. Crawshaw, Eur. Phys. J. E **26**, 63 (2008).
82. N. Saitô, K. Takahashi, Y. Yunoki, J. Phys. Soc. Jpn. **22**, 219 (1967).
83. L.M. Bergström, *Thermodynamics of Self-Assembly* (INTECH, 2011).
84. P.J. Flory, J. Chem. Phys. **10**, 51 (1942).
85. M.L. Huggins, J. Chem. Phys. **9**, 440 (1941).
86. P.J. Flory, *Principles of Polymer Chemistry* (Cornell University Press, 1953).
87. W.H. Beyer, *CRC Standard Mathematical Tables*, 25th edition (1978).
88. H. Jung, B. Coldren, J. Zasadzinski, D. Iampietro, E. Kaler, Proc. Natl. Acad. Sci. U.S.A. **98**, 1353 (2001).
89. M.P. Do Carmo, *Differential Geometry of Curves and Surfaces* (Prentice-Hall Englewood Cliffs, 1976).